Synthetic and Systems Biotechnology 10 (2025) 226–236

Contents lists available at ScienceDirect

Synthetic and Systems Biotechnology

journal homepage: www.keaipublishing.com/en/journals/synthetic-and-systems-biotechnology

Original Research Article

Engineered probiotic-mediated intratumoral delivery and controlled release of bacterial collagenase for cancer therapy

Hong-Rui Li, Bang-Ce Ye *

Laboratory of Biosystems and Microanalysis, State Key Laboratory of Bioreactor Engineering, East China University of Science and Technology, Shanghai, 200237, China

ARTICLE INFO

Keywords:
Bacterial therapy
Extracellular matrix
Collagenase
Immunotoxin
Chemotherapy
Breast cancer

ABSTRACT

Elevated collagen levels within breast tumors are strongly associated with tumor progression and present a barrier to effective therapeutic agent penetration within the tumor microenvironment (TME), leading to poor clinical outcomes. To address this challenge, we engineered a probiotic strain to degrade collagen within the TME by selectively colonizing in tumors and releasing bacterial collagenase in a lysis-dependent manner. Initially, we constructed a therapeutic bacterial strain designed to lyse within the TME and release an encoded immunotoxin comprising a nanobody targeting CD47 (CD47nb) and a modified *Pseudomonas* exotoxin A (PE38KDEL). The introduction of collagenase-expressing bacteria, in conjunction with therapeutic immunotoxin, reduced collagen fiber levels within the TME, resulting in inhibited tumor growth and prolonged survival in a murine model of breast cancer. Furthermore, we investigated the broader applicability of the collagenase-expressing bacterial strain in combination with chemotherapeutic drugs, such as doxorubicin. Remarkably, synergistic antitumor effects were observed in mice treated with this combination therapy. In conclusion, our study demonstrates that probiotic delivery of bacterial collagenase offers a promising adjuvant treatment strategy for selectively degrading intratumoral collagen, thereby improving the efficacy of anticancer therapies in breast cancer.

1. Introduction

Breast cancer stands out as the most prevalent malignancy among women [1]. The extracellular matrix (ECM), a pivotal component of the breast TME, comprises a dynamic molecular network, including molecules like collagen and hyaluronic acid (HA), which are secreted by stromal or tumor cells [2,3]. The hallmark of malignant tumors often includes a significant increase in collagen deposition and cross-linking within the ECM [4]. This dense ECM acts as a barrier, limiting the penetration of therapeutic agents and the infiltration of immune cells into tumor tissues. Consequently, effective treatment often requires potentially toxic drugs to be administered at higher doses and more frequently [3]. To address this challenge, strategies aimed at enhancing the permeability of tumor tissues by breaking down ECM components have been explored, facilitating the migration and infiltration of drugs and immune cells into tumors, thereby enhancing the antitumor effect [5,6].

Collagen, being the most abundant protein in the ECM, has been a focus of research, and various collagenase enzymes have been investigated to improve the intratumoral distribution and efficacy of anticancer drugs in preclinical settings. For instance, systemic administration of collagenase has been shown to reduce interstitial fluid pressure (IFP) and temporarily increase the transcapillary pressure gradient, allowing monoclonal antibodies to penetrate deeper into tumors [7]. In experimental murine models, local treatment of peritoneal metastases of colorectal origin with intraperitoneal collagenase has demonstrated potential in enhancing the effectiveness of chemotherapy drugs administered both intravenously and intraperitoneally [8]. Additionally, collagenase has been utilized to modulate tumor ECM to facilitate the penetration of drug-loaded nanoparticles for enhanced chemotherapy [9]. However, challenges remain, including the risk of circulating bacterial collagenase leading to unnecessary degradation of collagen in normal tissues and the potential development of anti-collagenase antibodies that could neutralize bacterial collagenase and potentially cross-react with human matrix metalloproteinases [10,11]. Therefore, optimizing the efficacy and safety of collagenase treatment warrants further exploration.

Immunotoxins represent a class of tumor-targeting therapeutics

Peer review under responsibility of KeAi Communications Co., Ltd.
* Corresponding author.
E-mail address: bcye@ecust.edu.cn (B.-C. Ye).

https://doi.org/10.1016/j.synbio.2024.09.001
Received 25 June 2024; Received in revised form 24 August 2024; Accepted 3 September 2024
Available online 6 September 2024

composed of a specific targeting domain and a biological toxin through genetic recombination. Commonly, antibody fragments and receptor-binding ligands serve as the targeting domains of immunotoxins, with bacterial *Pseudomonas aeruginosa* exotoxin (PE) being one of the most potent toxin fusion partners due to its ability to inhibit protein synthesis and other unique advantages [12,13]. Despite the preclinical and clinical evaluation of PE-based immunotoxins and their approval for clinical application, non-specific toxicity and immune responses against immunotoxins continue to restrict their successful clinical applications [13,14]. Therefore, improving the delivery of immunotoxins represents an ideal direction to overcome these limitations.

Immunotherapy was first systematically studied as a potential treatment for malignant tumors over 100 years ago, when William B. Coley treated inoperable cancer patients by injecting Streptococcus and Coley's toxins. Various facultative anaerobes and obligate anaerobes, including *Escherichia coli* [15–17], *Clostridium* [18], *Bifidobacterium* [19] and *Salmonella* [20,21], have demonstrated tumor-targeting or tumor-killing activities. Therapeutic approaches based on tumor-targeting bacteria have significant advantages. Bacteria can enhance antitumor immune responses by preferentially accumulating within tumors [20,22,23]. When flexibly designed and modified, bacteria can also serve as vehicles for delivering nucleic acids, proteins, and cytotoxic agents according to clinical requirements, with drug release properties that are controllable, localized, and sustained, making tumor-targeted bacteria an attractive therapeutic option to combine with other antitumor therapies [24]. Previous studies have shown that tumor-targeting *Salmonella typhimurium* expressing functional bacterial hyaluronidase can degrade HA deposited in tumors and facilitate the penetration of chemotherapeutic drugs in mouse tumor models [25,26].

In this study, we engineered a probiotic *E. coli* strain to express a heterologous bacterial collagenase, aiming to degrade collagen within the tumor ECM and enhance the efficacy of combined tumor therapy drugs. Our results demonstrate that this system enables the combined local delivery of the immunotoxin along with TME-remodeling bacterial lysis adjuvants, effectively suppressing tumor proliferation (Fig. 1). Furthermore, the collagenase-expressing EcN strain can serve as a synergistic anticancer therapeutic agent to facilitate the delivery of chemotherapeutic drugs (such as doxorubicin) throughout the tumor.

2. Results

2.1. Design and characterization of the CD47-specific immunotoxin

Design of the immunotoxin was based on a nanobody antagonist of

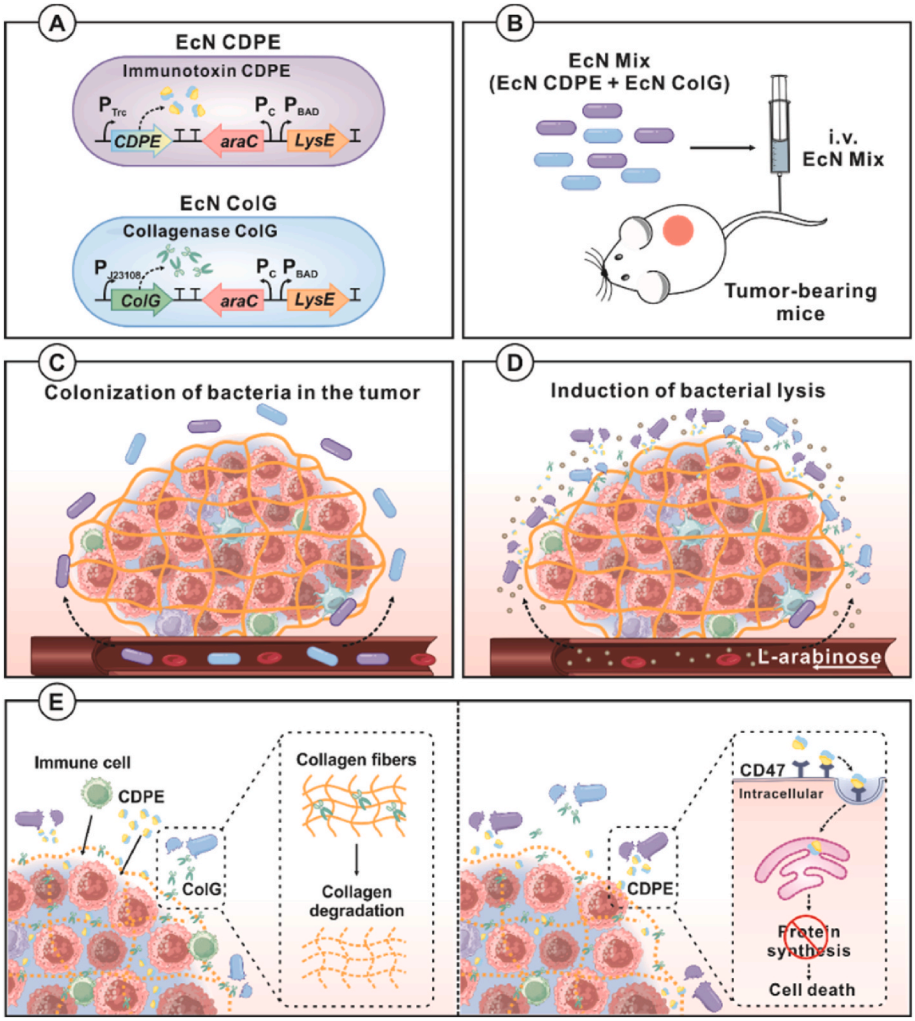

Fig. 1. The mechanism of cancer therapy with engineered EcN probiotics. (A) Plasmids were introduced into EcN in order to produce the EcN CDPE strain and the EcN ColG strain, enabling the bacteria to express immunotoxin CDPE or collagenase ColG controlled by constitutive promoters. (B) Dual engineered bacteria were injected intravenously into tumor-bearing mice. (C) After systemic administration, the bacteria selectively colonized the tumor. (D) EcN CDPE and EcN ColG expressed the bacteriophage lysis protein LysE following L-arabinose induction, leading to bacterial lysis and localized release of CDPE and ColG within the TME. (E) By breaking down collagen fibers in the structural components of the ECM, ColG facilitated the penetration and distribution of CDPE within the tumor. Concurrently, the delivery of CDPE, which inhibits protein synthesis in cells, directly targeted and killed tumor cells.

CD47 (CD47nb) and a truncated mutant form of *Pseudomonas* exotoxin A (PE38KDEL) [27]. CD47 is an innate immune regulator up-regulated in a wide range of tumor types that inhibit phagocytosis upon interaction with its receptor signal regulatory protein α (SIRPα) on macrophages. CD47nb shows particular valuable as therapeutic cargo, including SIRPα/CD47 antagonism, small size and allowing them to be produced recombinantly in bacteria [28,29]. PE38 is constructed by the removal of structural domain DIa and part of DIb of PE [12,13]. The carboxyl terminus RDEL motif of PE38 was replaced by KDEL, which enhances the endoplasmic reticulum localization of immunotoxins and correspondingly increases specific cytotoxicity [30,31]. CD47nb and PE38KDEL were linked by a flexible (G4S)3 linker to produce CD47nb-PE38KDEL (CDPE). We first evaluated the binding specificity of CDPE towards its corresponding receptor by ELISA assay, with BSA being used as the control protein. As shown in Fig. 2A, CDPE significantly bound to CD47, but not to BSA. To verify the binding of CDPE to tumor cells, 4T1 cells known to express CD47 were incubated with PE38KDEL or CDPE and then stained with a fluorescent-labeled antibody to detect bound toxins. We observed that the free toxin PE38KDEL did not specifically bind to 4T1 cells (Fig. 2B). In contrast, CDPE significantly bound to 4T1 cells, suggesting that CDPE can efficiently recognize 4T1 cells and that the binding of CDPE towards 4T1 cells was dependent on CD47nb. We then tested the cytotoxicity of CDPE to 4T1 cells in vitro. As shown in Fig. 2C, CDPE exhibited extremely strong cytotoxicity to 4T1 cells with an IC_{50} value as low as 0.10 nM. However, CD47nb and PE38KDEL showed much lower cytotoxic capacity, with 4T1 cell viability over 90 % when the concentration was increased up to 100 nM. These results confirmed that CDPE kills cells in a CD47nb-dependent manner. Moreover, the ability of CDPE to influence bone marrow-derived macrophages (BMDMs) phagocytosis of 4T1 cells was determined. CDPE treatment caused a ~60 % increase in phagocytosis, and treatment with CD47nb or PE38KDEL alone resulted in a 30–40 % increase in phagocytosis compared to PBS-treated cells (control) (Fig. 2D). Interestingly, the pretreatment of BMDMs with CD47nb or toxins did not induce phagocytosis of 4T1 cells compared with a PBS control (Fig. S1A). Furthermore, it was observed that both 100 nM of PE38KDEL and CDPE exhibited cytotoxicity on 4T1 cells, with CDPE displaying more potent cytotoxicity than PE38KDEL (Fig. S1B). The pretreatment of 4T1 cells with CD47nb and CDPE induced a similar increase in BMDM phagocytosis, suggesting that the binding of CD47nb and CDPE to the 4T1 cell surface CD47 may interrupt the CD47–SIRPα interaction [27]. Therefore, we speculate that CDPE enhances phagocytosis of tumor cells by macrophages in a combinatorial manner, namely through CD47 blockade as well as toxin-induced tumor cell damage [32].

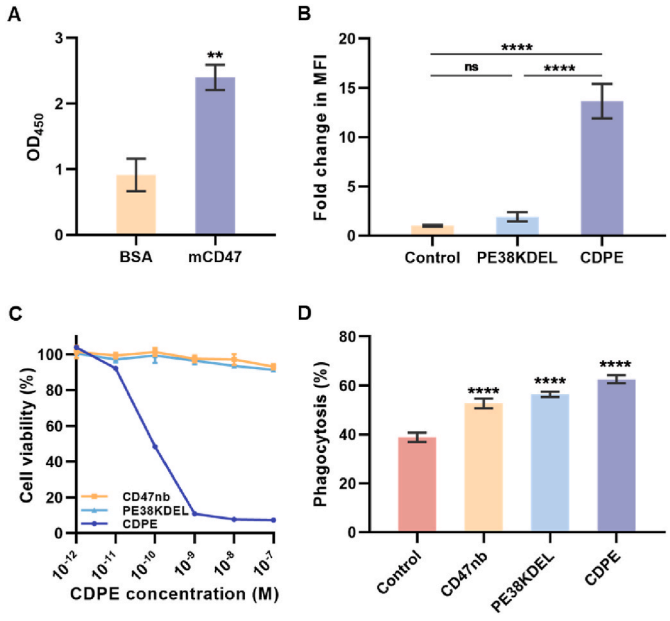

Fig. 2. Design and characterization of CD47-specific immunotoxin CDPE. (A) The binding specificity of CDPE to recombinant mouse CD47 and BSA (control) was analyzed by ELISA (**$P = 0.0012$, unpaired *t*-test). (B) The binding activity of CDPE and PE38KDEL to 4T1 cells was detected by flow cytometry. The negative control used only the CoraLite 647-conjugated anti-His-tag antibody as a detection antibody without incubation with nanobody or toxin. Mean fluorescence intensity (MFI) values are normalized to the mean MFI of the control. (****$P < 0.0001$, ns, not significant ($P > 0.05$); one-way ANOVA). (C) 4T1 cells were incubated with different concentrations of CD47nb, PE38KDEL or CDPE for 48 h, and cell viabilities were determined by CCK-8. (D) CFSE-labeled 4T1 cells and CMTPX-labeled BMDMs were co-cultured in the presence of CD47nb, PE38KDEL, CDPE or PBS (control), and the phagocytosis of 4T1 cells by BMDMs was determined by flow cytometry. Phagocytosis is quantified as the percentage of CMTPX-positive macrophages that have engulfed CFSE-positive 4T1 cells (****$P < 0.0001$, one-way ANOVA).

2.2. Characterization of the recombinant bacterial collagenase

Clostridium histolyticum collagenase, known as Xiaflex, has been employed as clinical trials for the treatment of Peyronie's disease and Dupuytren's contracture. Xiaflex is a mixture with a constant ratio of class I (AUX-I) and class II (AUX-II) collagenase which are encoded by two bacterial genes, *colG* and *colH* [33]. Based on the clinically proven of enzymatic collagenolysis, the collagenase ColG may be used for improving cancer therapy. We examined the collagenase activity of the heterologously expressed ColG from *E. coli*, using N-(3-[2-Furyl]-Acryloyl)-Leu-Gly-Pro-Ala (FALGPA) as a synthetic substrate, with heat-denatured ColG as a negative control, ColG showed FALGPA hydrolysis activity (Fig. 3A). The initial in vitro study on the effect of ColG on collagen in breast cancer cells indicated that the treatment with ColG on 4T1 cells resulted in a reduction in collagen expression of approximately 14 % (Fig. 3B and C). Next, we tested whether ColG treatment would increase the binding of CDPE to tumor cells. 4T1 cells were incubated with CDPE in the presence of ColG, and the bound CDPE were labeled with an antibody. As expected, we observed that ColG led to an increase of fluorescently labeled antibody, suggesting that ColG-mediated ECM degradation contributes to the cellular uptake of immunotoxin (Fig. 3D). Inhibition curves of CDPE obtained in the presence or absence of ColG were compared to determine the potency of ColG, as shown in Fig. 3E. The IC_{50} of CDPE in ColG showed a lower value (0.067 nM) than that in control. ColG alone did not shown cytotoxicity to 4T1 cells (Fig. S2).

2.3. Characterization of the engineered bacteria expressing CDPE or ColG

After confirming properties of CDPE and ColG, the coding sequences were cloned into separate plasmids under the control of constitutive promoters to allow for moderate gene expression. A bacteriophage lysis protein, LysE, was added downstream of a P_{BAD} promoter on these vectors for inducing bacterial lysis to release protein drugs from *E. coli*, and a chromosome-plasmid balanced lethal system was also separately cloned into each of the two plasmids owing to plasmid stability. These plasmids were then transformed into engineered EcN, respectively. Bacterial growth dynamics of CDPE-expressing-EcN (EcN CDPE) and ColG-expressing-EcN (EcN ColG) showed that most bacteria lysed following L-arabinose induction (Fig. 4A). Western blot analysis of the presence of CDPE or ColG in concentrated bacterial culture supernatants and cell pellets indicated that CDPE and ColG were successfully expressed in EcN and released upon bacteria lysis (Fig. 4B). Further analyses demonstrated that bacterial cell-free supernatants containing active CDPE could reduce the 4T1 cell viability (Fig. 4C). Subsequently, we explored the collagen-depletion efficacy of EcN ColG in vivo. Masson's trichrome staining of tumors dissected from mice that had been separately treated with PBS, EcN or EcN ColG showed a significant

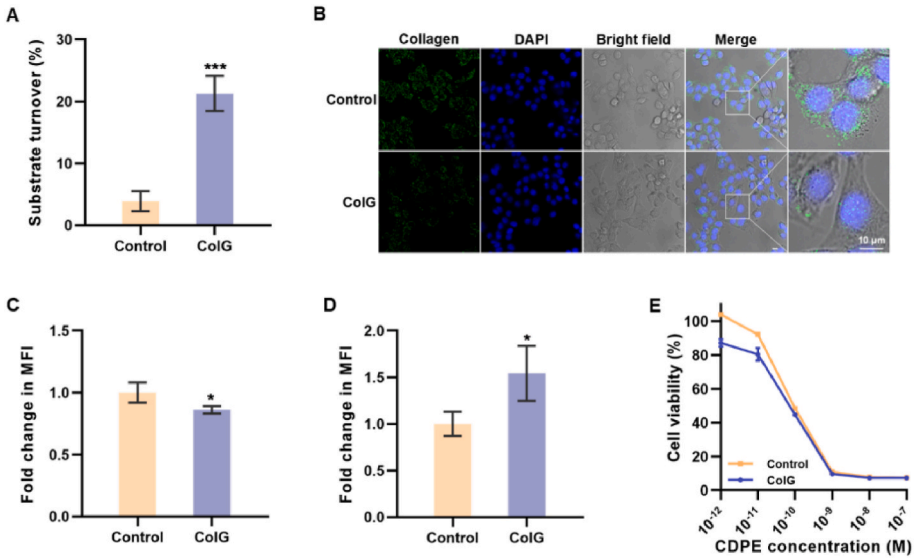

Fig. 3. Characterization of recombinant collagenase ColG. (A) Enzymatic assay of collagenase using FALGPA as a substrate with heat-denatured ColG as a negative control (***$P = 0.0008$, unpaired *t*-test). (B) Confocal images of collagen I stained by anti-collagen I antibody in 4T1 cells after active ColG and heat-denatured ColG (control) treatments (scale bar = 10 μm). DAPI indicates the cell nucleus. (C) Flow cytometric analysis of collagen in 4T1 cells after different treatments. Heat-denatured ColG was used as a control. MFI values are normalized to the mean MFI of the control group. (*$P = 0.0486$, unpaired *t*-test). (D) Binding ability of CDPE to ColG-treated 4T1 cells was detected by flow cytometry. MFI values are normalized to the mean MFI of the untreated control cell group. (*$P = 0.0433$, unpaired *t*-test). (E) 4T1 cells were incubated with different concentrations of CDPE for 48 h with or without the presence of ColG, and cell viabilities were determined by CCK-8. Serial dilutions of heat-denatured ColG were used as a control.

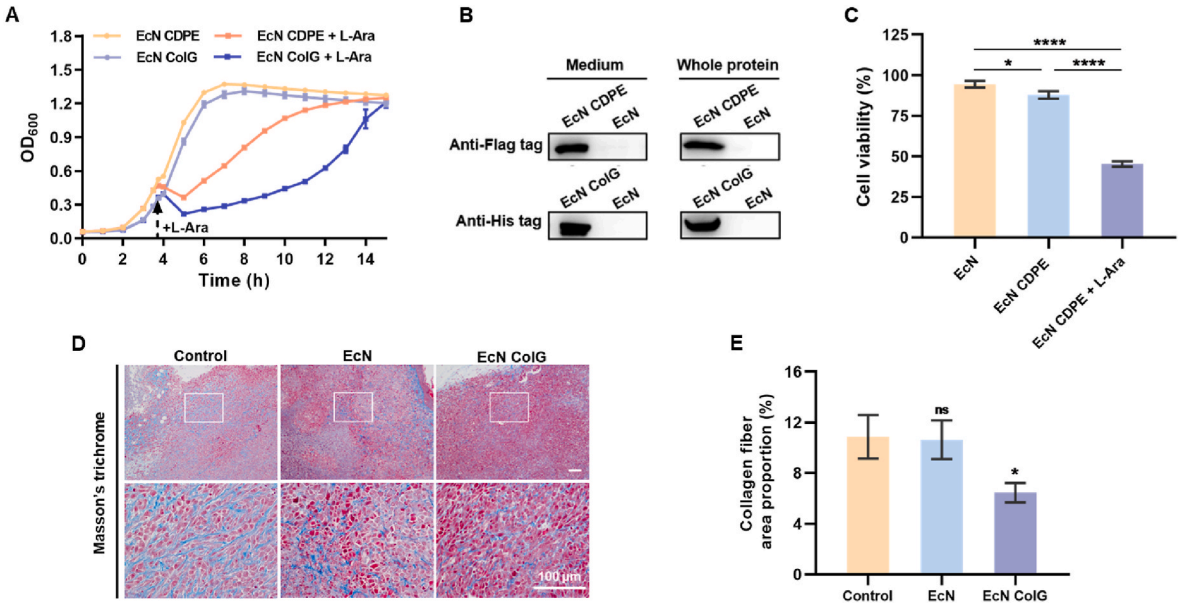

Fig. 4. Characterization of engineered bacteria. (A) Bacterial growth dynamics of EcN CDPE and EcN ColG in LB culture. EcN CDPE was cultivated at 37 °C and induced with 12 mM L-arabinose until OD_{600} become ~0.4. (B) The presence of CDPE or ColG in bacterial culture supernatants and cell pellets was visualized by western blot using anti-Flag tag antibody or anti-His tag antibody. (C) 4T1 cells were co-incubated with diluted bacterial supernatants that contained lysis-dependent released CDPE. Cell viabilities were determined by CCK-8 (****$P < 0.0001$, *$P = 0.0173$; one-way ANOVA). (D) 4T1 tumor-bearing mice received intravenous injections every 3 days with PBS, EcN or EcN ColG, and L-arabinose was intraperitoneally injected at 48 h post bacteria treatments. Tumors were collected and subjected to Masson's trichrome staining on day 15 (scale bar = 100 μm). (E) The area ratios of collagen fibers in Masson's trichrome staining sections were quantified by Image J (n = 3 per group, *$P = 0.0195$, ns, not significant ($P > 0.05$); one-way ANOVA). Collagen fiber (%) = A_0(type I collagen area)/A_1(total tissue area) × 100 %.

decrease in intratumoral collagen fibers in EcN ColG-treated 4T1 tumors (Fig. 4D and E).

2.4. Tumor-targeting and biosafety of the engineered bacteria

For non-invasive live detection of the tumor-targeting ability of EcN as a delivery vector in bacterial therapy, the EcN lux strain containing the *luxCDABE* operon was injected intravenously into 4T1 tumor-bearing mice. Injection of EcN lux immediately resulted in a strong bioluminescence signal localized mainly in the liver, followed by a detectable bioluminescence signal in the tumor of the same mouse 48 h after injection (Fig. 5A). Notably, no signal was observed at 24 h post

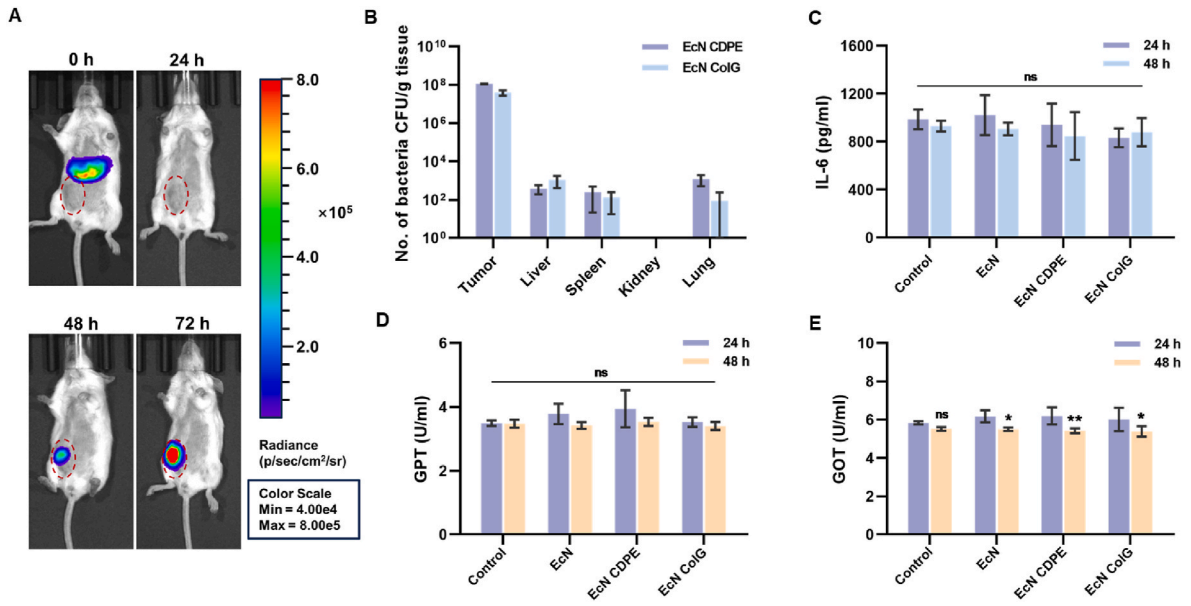

Fig. 5. Tumor-targeting ability and biosafety assessment of bacterial therapy. (A) IVIS images showing changes in bacterial bioluminescence over time for EcN lux. (B) Distribution and tumor colonization of EcN CDPE and EcN ColG in 4T1 tumor-bearing BALB/c mice. The mice were euthanized, and the tumors and major organs were homogenized, diluted, and analyzed for the presence of bacteria at 24 h post injection by plate count. (C–E) Serum analysis of IL-6 (n = 3 per group, ns, not significant ($P > 0.05$); two-way ANOVA), GPT (n = 4 per group, ns, not significant ($P > 0.05$); two-way ANOVA) and GOT (n = 4 per group, $^{**}P = 0.078$, $^{*}P < 0.05$, ns, not significant ($P > 0.05$); two-way ANOVA) in mice at 24 h and 48 h after intravenous injection of bacteria.

injection. In light of the potential limitation of the *luxCDABE* promoter strength, this result did not reveal the absence of EcN lux in tumor tissues. The results of the bacterial count using homogenized tumors and major organs further indicated that the significant accumulation of engineered EcN in tumors, but not in other organs, was detectable as early as 24 h post injection (Fig. 5B). To examine whether TME-targeting EcN had a good biosafety in vivo, the blood of 4T1 tumor-bearing mice 24/48 h after injection of engineered EcN was collected for serum biochemical and cytokine analysis. In contrast, the engineered EcN had no significant abnormalities post injection (Fig. 5C–E). For long-term biosafety evaluation, major organs in mice were collected for HE staining and histopathological analysis after 15 days treatment. No evidence of frank necrosis was observed in major organs from the bacteria treatment groups (Fig. S3). All groups had mice with mild inflammatory infiltrates in the lungs and livers. These minimal infiltrates were classified as background lesions and were deemed unrelated to bacteria treatments. The intravenous infusion of bacteria did not cause any significant inflammatory responses in the spleen or kidneys. Taken together, the results demonstrate the good biosafety of engineered EcN for antitumor therapy.

2.5. Antitumor effects of the engineered bacteria in vivo

The advantages of our proposed therapeutic protein-expressing EcN strains include their efficacy in specifically degrading collagen in the TME and suppressing tumor proliferation with the combination therapy of EcN CDPE and EcN ColG. Therefore, we sought to characterize the therapeutic effect in 4T1 tumor-bearing mice, and the treatment schedule is shown in Fig. 6A. Among the mice treated with EcN Mix, in which the bacterial suspension for intravenous injection was mixed with EcN CDPE and EcN ColG in an equal (1:1) ratio, tumor growth exhibited a significant reduction compared with other groups (Fig. 6B). Monotherapy treatment of EcN CDPE slightly reduced tumor growth in 4T1 tumor-bearing mice, while tumor growth was not significantly suppressed in the EcN ColG group. IHC staining of Ki67 protein, a marker of cell proliferation activity in tumors, showed that the treatment of EcN CDPE or EcN ColG alone decreased the number of Ki67-positive cells in tumors (Fig. 6C). Additionally, the number of Ki67-positive cells was further decreased in the EcN Mix-treated group. These results were also confirmed by the semiquantitative analysis of Ki67-positive area proportion (Fig. 6D). Masson's trichrome staining analysis of tumors revealed that the collagenase ColG expressed by EcN ColG or EcN Mix decreased the level of collagen fibers in the TME (Fig. 6C and E). Tumor immunity relies on immune mediators like IFN-γ, which is secreted primarily by activated lymphocytes to the TME for underlying antitumorigenic effects. The results from ELISA showed that the expression of IFN-γ in tumor tissues increased significantly in the EcN Mix group compared with other groups (Fig. 6F), which indicated that the combination therapy of EcN CDPE and EcN ColG possibly enhanced the antitumor immune response and modulated the TME. Moreover, survival assays showed that treatment with EcN Mix slightly prolonged the survival of 4T1 tumor-bearing mice (Fig. 6G). During treatments, the body weight of each mouse was assessed every 2 days to evaluate bacterial tolerance under treatments. The results showed no significant differences in body weight between each group (Fig. 6H). Overall, these results and analyses indicated that the combination therapy of EcN CDPE and EcN ColG can safely degrade collagen in the tumor region and inhibit the proliferation activity of the tumor.

2.6. Tumor-suppressive effects of the combination therapy with collagenase-expressing bacteria and chemotherapeutic drug

To further explore the broader applicability of EcN ColG in combination with chemotherapeutic drugs, these 4T1 tumor-bearing mice were administered doxorubicin, EcN ColG, or the combination of doxorubicin and EcN ColG (Fig. 7A). Tumor growth was reduced in the group cotreated with doxorubicin and EcN compared to the group treated with doxorubicin alone (Fig. 7B). Although tumor growth in mice simultaneously administered doxorubicin and EcN ColG was not statistically different from that in mice cotreated with doxorubicin and EcN in the initial phase of treatment, the combined administration of doxorubicin and EcN ColG finally slowed tumor growth. Determination of the number and proportion of proliferative tumor cells by Ki67 IHC analysis revealed a lower percentage of Ki67-positive cells in tumors following the combined treatment with doxorubicin and EcN ColG compared to the combined treatment with doxorubicin and EcN (Fig. 7C

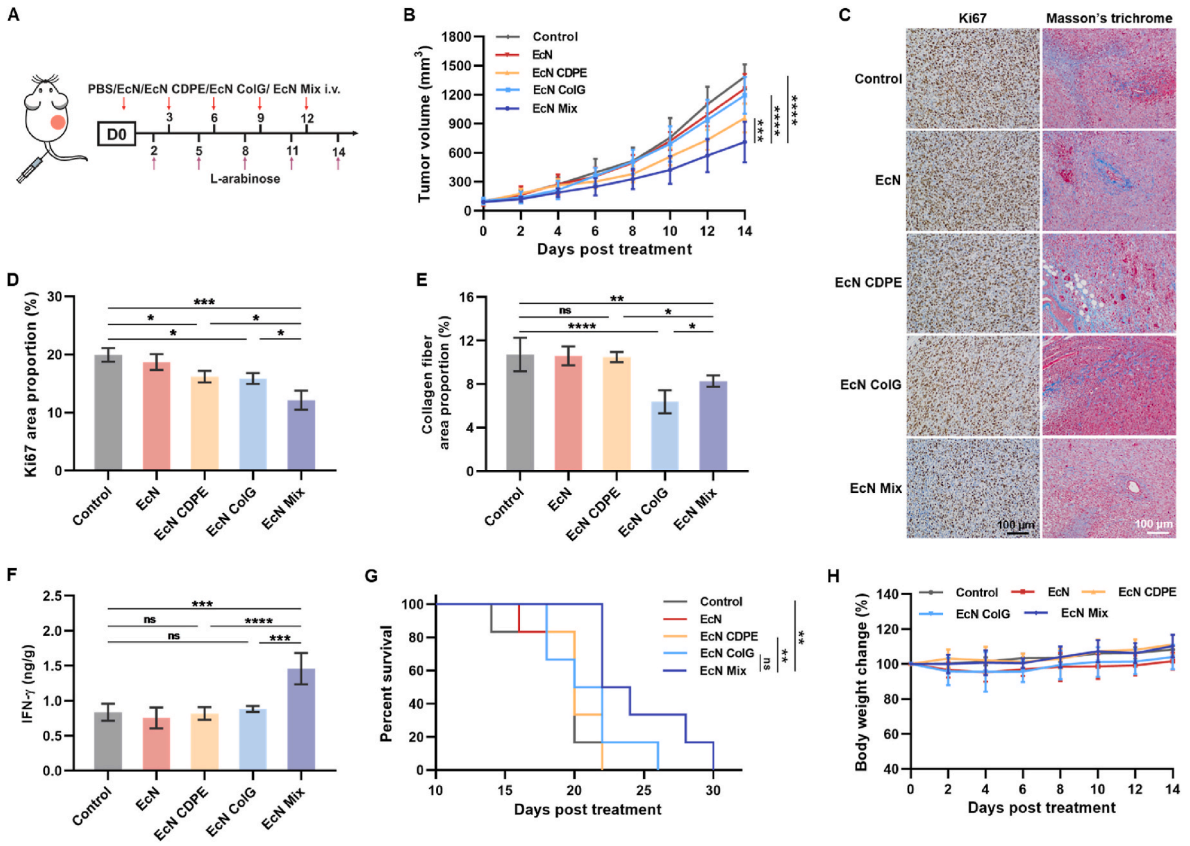

Fig. 6. Antitumor effects of bacterial therapy in vivo. (A) Treatment schedule. 6-8-week-old female BALB/c mice were implanted with 2.5×10^5 4T1 cells. After tumor volumes reached approximately 60–100 mm^3, mice were intravenously injected with PBS, EcN, EcN CDPE, EcN ColG or EcN Mix (EcN CDPE and EcN ColG at a ratio of 1:1) every 3 days. L-arabinose was intraperitoneally injected at 48 h post bacteria injection to induce the lysis-dependent release of therapeutic proteins. Tumors from each group were isolated and analyzed on day 15. (B) Tumor growth curves (n = 6 per group, $^{****}P < 0.0001$, $^{***}P = 0.0005$; two-way ANOVA). (C) IHC assay of Ki67 expression and Masson's trichrome staining of collagen fibers in tumor tissues (scale bar = 100 μm). (D) Quantitative analysis of Ki67-positive cells in the tumor areas measured by Imgae J (n = 3 per group, $^{***}P = 0.0001$, $^{*}P < 0.05$; one-way ANOVA). (E) The proportions of collagen fibers in the Masson's trichrome images of each group were quantified by Image J (n = 4 per group, $^{****}P < 0.0001$, $^{**}P = 0.0095$, $^{*}P < 0.05$; one-way ANOVA). (F) Tumors were homogenized, and the homogenate supernatants were analyzed for IFN-γ by ELISA (n = 4 per group, $^{****}P < 0.0001$, $^{***}P < 0.001$, ns, not significant ($P > 0.05$); one-way ANOVA). (G) Survival curves for 4T1 tumor-bearing mice (n = 6 per group, $^{**}P < 0.01$, ns, not significant ($P > 0.05$); log-rank test). (H) Relative body weight of 4T1-tumor-bearing mice with different treatments (n = 6 per group).

and D). The degradation of collagen within the TME was reflected by Masson's trichrome staining (Fig. 7C and E). The results suggested that EcN ColG degraded tumor-associated collagen fibers in chemotherapy. To further observe whether the decreased level of collagen using EcN ColG leads to tumor accumulation of doxorubicin, doxorubicin autofluorescence at the tumor site was detected by fluorescence microscopy. In the combination therapy group of EcN and doxorubicin, there was a minor increase in red fluorescence, which was more intense compared to the doxorubicin monotherapy group (Fig. S4A). Doxorubicin fluorescence was most intense in the EcN ColG combination group, indicating successful tumor infiltration with doxorubicin after EcN ColG treatment (Figs. S4A and S4B). The combination of EcN ColG and doxorubicin resulted in a significant increase in intratumoral IFN-γ (Fig. 7F). These results suggested that this treatment may have improved immune-mediated tumor regression in the TME, thereby contributing to the efficacy of tumor therapy. Mice treated with doxorubicin, EcN plus doxorubicin, or EcN ColG plus doxorubicin exhibited a significantly prolonged survival time compared to the control group (Fig. 7G). Notably, the combination therapy of doxorubicin and EcN ColG induced the highest survival rate of mice among treatments at the end of the experiment. All the mice tolerated the combination of doxorubicin and the probiotic therapy, as evidenced by no observed differences in mouse body weight between the chemotherapy groups (Fig. 7H). Taken together, these data proved the efficacy and safety of the combination therapy with the collagenase-expressing EcN and doxorubicin.

3. Discussion

We established a strategy for the expression and local delivery of a heterologous bacterial collagenase by a probiotic *E. coli* strain for cancer therapy, allowing for the combination of local delivery of the immunotoxin or systemic administration of chemotherapeutic drugs along with the TME-remodeling bacterial adjuvant. We have demonstrated that the intravenous administration of the collagenase-expressing EcN strain results in the degradation of collagen within the TME, thereby enhancing the penetration and antitumor efficacy of combined tumor therapy drugs.

Excessive production of collagens, which is one of the main pathological features of some cancers, contributes to several limitations of antitumor therapeutic applications [34]. Previous reports show that treatment with collagenase increased the diffusion and penetration of drugs into the treated tumor but remains controversial due to the off-target toxicity and the immunogenicity of bacterial collagenases following systemic administration [7,11,35]. To reduce the risks of toxicity from collagen breakdown in healthy tissues, we engineered EcN ColG that selectively colonizes tumors to locally release high effective concentration of the collagenase ColG. After intravenous injection with EcN ColG, we found a significant accumulation of EcN ColG in tumors

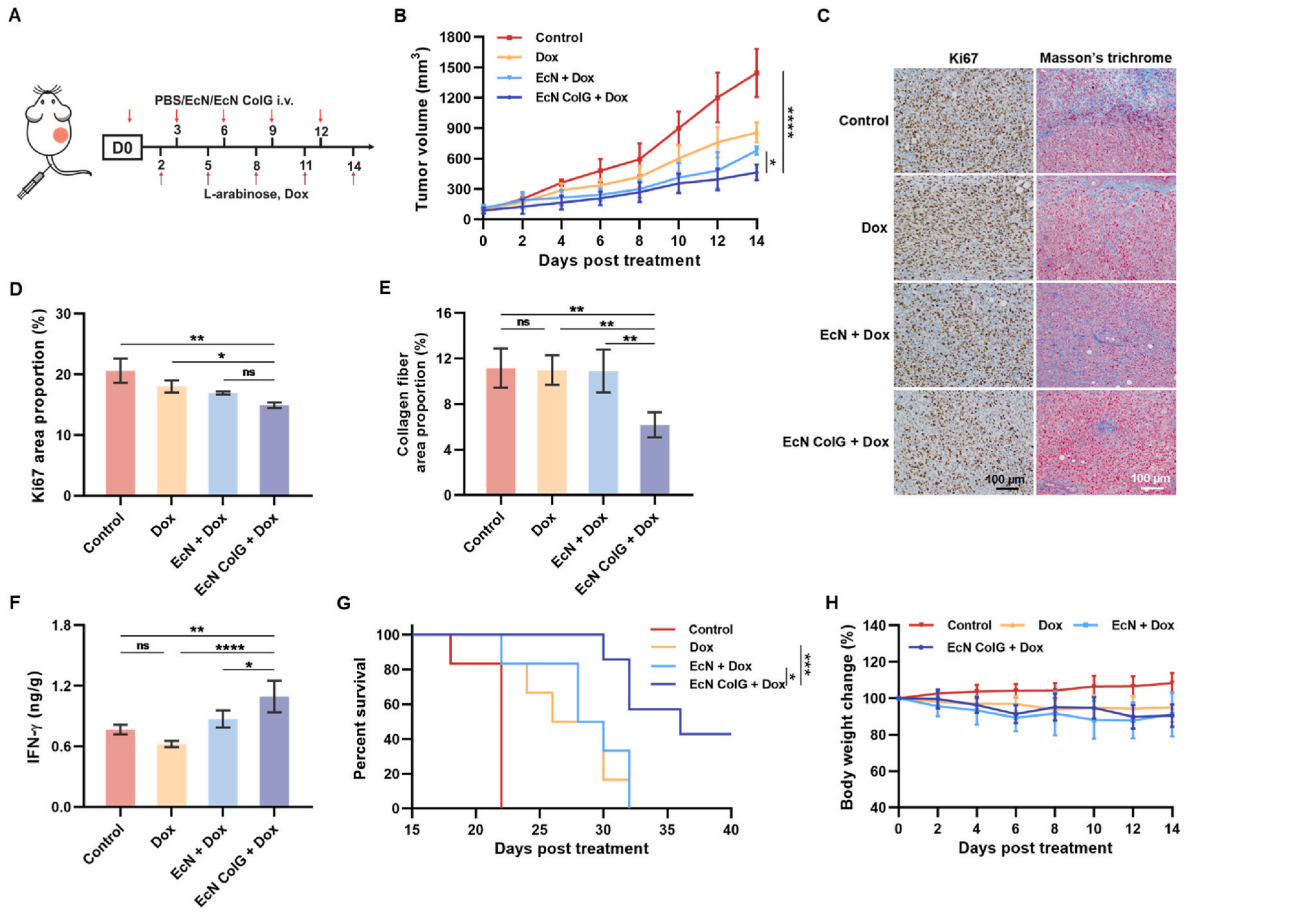

Fig. 7. Combination therapy with collagenase-expressing bacteria and chemotherapeutic drug. (A) Treatment schedule. 6-8-week-old female BALB/c mice were implanted with 2.5×10^5 4T1 cells. After tumor volumes reached approximately 60–100 mm^3, mice were intravenously injected with PBS, EcN, or EcN ColG every 3 days. L-arabinose was intraperitoneally injected at 48 h post bacteria injection to induce the lysis-dependent release of therapeutic protein. Then, the animals were intravenously injected with doxorubicin 3 h after protein expression induction. Tumors from each group were isolated and analyzed on day 15. (B) Tumor growth curves (n = 6 per group, $^{****}P < 0.0001$, $^{*}P = 0.0114$; two-way ANOVA). (C) IHC assay of Ki67 expression and Masson's trichrome staining of collagen fibers in tumor tissues (scale bar = 100 μm). (D) Quantitative analysis of Ki67-positive cells in the tumor areas measured by Imgae J (n = 3 per group, $^{**}P = 0.0014$, $^{*}P = 0.0441$, ns, not significant ($P > 0.05$); one-way ANOVA). (E) The proportions of collagen fibers in the Masson's trichrome images of each group were quantified by Image J (n = 4 per group, $^{**}P < 0.01$, one-way ANOVA). (F) Tumors were homogenized and the homogenate supernatants were analyzed for IFN-γ by ELISA (n = 4 per group, $^{****}P < 0.0001$, $^{**}P = 0.0016$, $^{*}P = 0.0243$, ns, not significant ($P > 0.05$); one-way ANOVA). (G) Survival curves for 4T1 tumor-bearing mice (n = 6 per group, $^{***}P = 0.0006$, $^{*}P = 0.0110$, ns, not significant ($P > 0.05$); log-rank test). (H) Relative body weight of 4T1-tumor-bearing BALB/c mice with different treatments (n = 6 per group).

but not in other organs. In this study, EcN ColG has been demonstrated to significantly reduce intratumoral collagen fibres, making it a highly modular adjuvant therapeutic bacterial strain, potentially enabling multiple forms of combination therapy. Therefore, we explored the antitumor effects of the tumor-colonizing EcN CDPE strain, which specifically lyses within the TME and in situ releases of the immunotoxin CDPE, in combination with the EcN ColG strain. The immunotoxin CDPE, consisting of a CD47 nanobody fused to a truncated mutant form of PE toxin, showed extremely strong cytotoxicity to tumor cells in this study. Moxetumomab pasudotox is a recombinant CD22-targeting immunotoxin based on the PE toxin that received its first global approval for the treatment of hairy cell leukaemia. The intravenous administration of Moxetumomab pasudotox was associated with the development of hemolytic uremic syndrome and capillary leak syndrome in patients [36]. In this study, the tumor-colonizing probiotic EcN and a bacterial lysis-release system were used to regulate the release of CDPE for minimizing systemic toxicity. The EcN CDPE strain was induced and released CDPE as it accumulated and proliferated within the tumor at 48 h post treatments. The nanobody of CDPE binds to CD47, a cell surface receptor expressed in a wide range of tumor types, thereby delivering CDPE directly to tumor cells. This is why a good biosafety of engineered EcN was observed during treatments. Regarding the broader applicability of EcN ColG in combination with chemotherapeutic drugs, we have demonstrated that the combination therapy of EcN ColG and doxorubicin exhibited a significant reduction of tumor growth compared with other groups. EcN treatment successfully improved the tumor infiltration with doxorubicin. Preclinical studies investigating the potential of collagenases in oncology have demonstrated that collagenase treatment enhances the diffusion and penetration of proteins, nanoparticles and lipoplexes within treated tumors [11]. Consequently, pretreatment or combined treatment with EcN ColG may improve therapeutic efficacy when used alongside immune checkpoint inhibitors, chemotherapeutic agents, or nanoparticles for stroma-dense, treatment-resistant cancers.

Tumor development, metastasis and therapeutic resistance are substantially influenced by the TME, making targeted therapies that aim to re-modulate the TME an attractive strategy for improving current treatments. Bacteria possess the distinctive capacity to selectively target the TME and deliver cancer therapeutics in a controlled manner, upon which they have been genetically engineered in various ways as therapeutic vehicles. TME-targeted bacteria-based cancer therapies have been designed to address both cellular and non-cellular factors, with the

goal of modulating the TME. For non-cellular factors, such as cytokines, aberrant vasculature, hypoxia, acidosis, and overexpression of ECM enzymes, engineered bacteria can change the TME through different mechanisms. For example, a *Salmonella typhimurium* strain delivering anti-angiogenic agent endostatin suppressed tumor angiogenesis and growth [37]. Similarly, it was reported that hyaluronidase-expressing *Salmonella typhimurium* effectively degraded HA in tumors and inhibited the interaction between CD44 and HA in vivo, which is synergistic with chemotherapy [29]. When *Shewanella oneidensis* MR-1 surface was supplemented with MnO_2 nanoflowers and modified as a lactate-fueled biohybrid, this biohybrid exhibited the capacity to directly catabolize lactate and indirectly relieve lactate production by downregulating HIF-1α expression [38]. Despite the encouraging progress of bacterial therapy in tumor-targeted delivery, several remaining challenges must be addressed to make the therapy more clinically-relevant, including limiting bacterial virulence and ensuring effective bacterial colonization. One common strategy to reduce the toxic side effects of bacterial vehicles is attenuation. The recombinant-attenuated bacteria can be obtained through screening of strains with different virulence phenotypes or construction of strains with auxotrophic mutations, which allow preferential acquisition of specific growth factors from the TME and proliferation in tumors. Encapsulating bacteria with tunable and dynamic expression of surface capsular polysaccharides also develops the biocompatibility of bacteria. However, excessive attenuation may decrease the bacterial colonization rate and intrinsic immunogenicity. Bacterial colonization in tumors increased with greater motility, and motility influenced the spatial distribution of bacterial accumulation within tissues, with motile strains penetrating more deeply [39]. Consequently, researchers can improve the motility of bacterial vehicles to achieve the balance between bacterial colonization and attenuation.

In this work, we generated an EcN strain that enhances the degradation of collagen within the TME by selectively colonizing tumors and releasing bacterial collagenase ColG in a lysis-dependent manner. The collagenase-expressing EcN showed synergistic antitumor effects with the similarly engineered EcN, which controllably released immunotoxin CDPE. The combination therapy of doxorubicin and the collagenase-expressing EcN inhibited tumor growth and prolonged survival in a mouse model of breast cancer. The present results and previous work have showed a dramatic improvement in antitumor therapy following collagen depletion, but the systemic off-tumor toxicity and immunogenicity of administered collagenase need to be carefully addressed. In situ delivery of bacterial collagenase by EcN could provide a potential adjuvant treatment to selectively degrade intratumoral collagen, further enhancing bacterially mediated therapeutics and overcoming the limitations of chemotherapy.

4. Materials and methods

4.1. Cell lines and animal models

The 4T1 mammary carcinoma cells were obtained from the Typical Culture Preservation Commission Cell Bank of the Chinese Academy of Sciences (China). The cells were cultured in RPMI-1640 medium (Solarbio) supplemented with 10 % fetal bovine serum (Gibco), penicillin, and streptomycin at 37 °C and 5 % CO_2.

East China University of Science and Technology approved all animal protocols, and all experiments were performed in strict accordance with *the Guidelines for Care and Use of Laboratory Animals* [ECUST-21038]. 6-8-week-old female BALB/c mice were purchased from the Shanghai Model Organisms Center (China). 4T1 cells were implanted in the fourth mammary fat pads on one flank of the mice, with each implant containing of 2.5×10^5 cells. Tumors were grown to an average volume of approximately 60–100 mm^3 before treatment with doxorubicin or bacterial strains. Tumor volume and body weight were assessed every 2 days. Tumor volume was calculated by measuring the length and width of each tumor, where $V = (\text{length} \times \text{width}^2)/2$. Mice were euthanized when the tumor volume reached 2000 mm^3.

4.2. Strains and plasmids

Plasmids in this study were generated through homologous recombination. The collagenase gene *colG* from *C. histolyticum* and the immunotoxin CDPE-encoding gene were optimized for expressing in *E. coli* and chemically synthesized by RuiMian (Shanghai, China). Each gene of two different domains of CDPE, CD47nb and PE38KDEL, were linked by a flexible linker (G4S)3. The *colG* gene and CDPE-encoding gene, with an N-terminal pelB signal peptide, were individually driven by the promoters P_{J23108} and P_{Trc}. Lysin gene E (*LysE*) from bacteriophage ΦX1174 under the control of the P_{BAD} promoter, amplified from a pWT-atgE-BE-AvG plasmid [40]. Next, the ColG genic region, with a 6 × His-tag fused to the C-terminus, and the LysE region were inserted into a pET28a plasmid to obtain the plyColG plasmid for the constitutive expression of ColG. The CDPE genic region with a C-terminal Flag-tag and the identical LysE region were inserted into a pTrcHisA plasmid to construct the CDPE constitutive expression vector, named plyCDPE. The *lacI* gene was removed from both of the plasmids mentioned above. To show bacterial distribution in vivo, the *luxCDABE* operon from *Photorhabdus luminescens* was constructed into a pET28a vector to form the pET28a-lux plasmid. The essential *glnA* gene-based chromosome--plasmid balanced lenthal system was introduced into EcN and plasmids described above to minimize plasmid loss in vivo. EcNΔ*glnA* cells were transformed with plasmids plyCDPE, plyColG or pET28a-lux, and designated as EcN CDPE, EcN ColG and EcN lux, respectively. Additionally, the *E. coli* codon-optimized sequences for CD47nb, PE38KDEL, CDPE and ColG were separately cloned into the NcoI and XhoI restriction sites upstream of the 6 × His tag of pET28a plasmid (pET28a-CD47nb, pET28a-PE38KDEL, pET28a-CDPE, pET28a-ColG), and all constructed plasmids were transformed into BL21 (DE3) *E. coli* cells for protein expression.

4.3. Protein expression and purification

For purification of CD47nb, PE38KDEL, CDPE and ColG, *E. coli* cells containing expression vectors were grown at 37 °C to an OD_{600} of approximately 0.4–0.6 and induced with 0.5 mM IPTG at 20 °C overnight. Cells were harvested by centrifugation. After washing twice with cold PBS, the cells were resuspended and sonicated in lysis buffer (35 mM imidazole, 50 mM NaH_2PO_4, 300 mM NaCl, pH 8.0), and lysates were centrifuged at 8000 r.p.m. for 20 min at 4 °C. The supernatants were loaded onto Ni-NTA resin (TransGen) and washed in wash buffer containing 20 mM imidazole, followed by elution in a high imidazole buffer (250 mM imidazole). The purified proteins, which were concentrated and washed at least twice with PBS using Amicon Ultra centrifugal filter, were collected and quantified by the bicinchoninic acid (BCA) assay (Beyotime). Bacterial endotoxin was removed from the purified proteins by consecutive wash steps with Triton-114.

4.4. Binding specificity analysis of CDPE

For CDPE ELISA analysis, ELISA plates were coated overnight at 4 °C with 100 nM recombinant mouse CD47 (ABclonal) and BSA in PBS to allow for optimal protein adsorption. The wells were washed with PBST and blocked with 5 % BSA in PBST. Then 200 nM CDPE was added to the wells. Plates were incubated for 2 h and washed with PBST to remove unbound proteins. Bound CDPE was detected using a mouse anti-His tag antibody (TransGen) followed by incubation with an HRP-conjugated goat anti-mouse lgG (H + L) secondary antibody (TransGen). The tetramethylbenzidine (TMB) substrate (Yeasen) was added to each well to detect the reaction of HRP, and the reaction of HRP was stopped by the addition of sulfuric acid. Finally, absorbance values were quantified at 450 nm in microplate reader (BioTek). To investigate the binding specificity of CDPE to tumor cells, 4T1 cells were incubated with the

purified PE38KDEL and CDPE (100 nM). The cells were washed with ice-cold PBS and then incubated with CoraLite 647-conjugated anti-His tag antibody (Proteintech). After washing to remove unbound antibody, the fluorescence was analyzed by flow cytometry (CytoFLEX).

4.5. In vitro cytotoxicity assay

The cytotoxic activity of CD47nb, PE38KDEL, CDPE and ColG was determined by CCK-8 assay. 4T1 cells were seeded in 96-well plates at a density of 2500 cells/well. Purified CD47nb, PE38KDEL, CDPE and ColG at various concentrations were added to the plates, and the cells were incubated for 48 h under standard cell culture conditions. Cell viability of 4T1 cells was measured by CCK-8 reagent (Yeasen) according to the manufacturer's instructions. The percentage of cell viability was obtained by comparing the optical density (OD) values of the protein-treated group with the untreated group.

4.6. Phagocytosis assay

Bone marrow cells were isolated from the tibias and femurs of BALB/c mice by flushing the bones with complete DMEM medium. After collecting by centrifugation, cells were filtered through a 70 μm cell strainer. RBCs were lysed with lysis buffer (Solarbio). Cells were pelleted by centrifugation and resuspended in complete medium supplemented with 10 ng/ml M-CSF (PeproTech) and 1 % P/S. The culture medium was replenished every 2–3 days. On the day 7, BMDMs were collected by cell scraping and washed in serum-free DMEM for later use. To quantify immunotoxin-dependent macrophage phagocytosis in vitro, 4T1 cells and BMDMs were individually labeled with carboxyfluorescein succinimidyl ester (CFSE) (Yeasen) and CellTrace Red CMTPX (Yeasen). 4T1 cells and BMDMs were co-cultured for 2 h with 100 nM CD47nb, PE38KDEL, or CDPE at a density of 9×10^5 cells/ml (effector-to-tumor cell ratio of 2:1). Cells were analyzed by flow cytometry and the ratio of $CFSE^+$ BMDMs to total $CMTPX^+$ BMDMs was calculated. To determine the mechanism of the CDPE-mediated increase in phagocytosis, BMDMs were pretreated with 100 nM CD47nb, PE38KDEL, CDPE or PBS and co-cultured with 4T1 cells. Alternatively, 4T1 cells were pretreated with 100 nM CD47nb, CDPE or PBS and co-cultured with BMDMs. After 2 h co-incubation of 4T1 cells and BMDMs, cells were analyzed by flow cytometry. The cytotoxic effects were examined by incubating 4T1 cells with 100 nM CD47nb, PE38KDEL or CDPE in serum-free DMEM for 2 h, followed by CCK-8 assay.

4.7. Collagenase activity

The biological activity of the collagenase ColG was tested using N-(3-[2-Furyl]-Acryloyl)-Leu-Gly-Pro-Ala (FALGPA) (Sigma) as a synthetic substrate. Briefly, ColG was incubated with FALGPA in 48.3 nM tricine, 9.67 mM $CaCl_2$, 387 mM NaCl. Heat-denatured ColG was used as a control. The enzymes were analyzed at 0.06 mg/ml using a substrate concentration of 0.967 mM FALPGA in 100 μl reaction volume. The decrease in absorbance upon substrate cleavage was monitored at 345 nm in a kinetic mode for 24 min using a microplate reader. Under the same reaction conditions, ColH was performed to achieve complete substrate turnover (100 %). The substrate turnover of ColG was calculated normalized using the lowest substrate absorbance in the ColH-mediated reaction.

4.8. The effect of ColG on collagen in tumor cells

The 4T1 cells were seeded in 24-well plates and treated with 10 μg/ml ColG for 24 h. To localize collagen, cells were fixed with 4 % paraformaldehyde and permeabilized in PBS containing 0.1 % Triton X-100. The cells were then stained with anti-collagen I antibody (Abbkine) and Alexa Fluor 488-conjugated goat anti-mouse secondary antibody. Nuclei were revealed by staining with DAPI (Solarbio). Immunofluorescence images were acquired with a laser scanning confocal microscopy. To further quantify the effects of ColG on cellular collagen expression, 4T1 cells were treated with 10 μg/ml ColG for 24 h and collected by cell scraper. The cells were fixed with 4 % paraformaldehyde, permeabilized in PBS containing 0.1 % Triton X-100 and then stained with anti-collagen I antibody and Alexa Fluor 488-conjugated secondary antibody. The cells were analyzed by flow cytometry. To investigate whether tumor cells treated using recombinant collagenase can improve the cell binding affinity of CDPE, 4T1 cells were co-cultured with 100 nM CDPE and 50 μg/ml ColG for 3 h. The cells were washed with ice-cold PBS, and bound CDPE was labeled with CoraLite 647-conjugated anti-His tag antibody. After washing to remove unbound antibody, the fluorescence was analyzed by flow cytometry. The enhanced cytotoxic activity of CDPE caused by collagenase treatment was investigated by CCK-8 assay. In brief, 4T1 cells were co-cultured with CDPE and ColG (5 μg/ml) at 37 °C. After 48 h, the cytotoxic activity was measured by the above-described CCK-8 method.

4.9. Characterization of engineered bacteria

Engineered bacterial strains were cultured overnight in LB medium. The overnight cultures were diluted 1:100 in 5 ml of fresh medium. Bacteria were grown at 37 °C to an OD_{600} of approximately 0.4 and induced with 12 mM L-arabinose. The bacterial cultures collected at various stages of growth at regular time intervals were added to 96-well plates, and the absorbance values of the medium were quantified at 600 nm using a microplate reader to assess the bacterial growth dynamics. After 12 h of incubation, the bacterial cultures were centrifuged, and the supernatants were concentrated using Amicon Ultra centrifugal filters. The pelleted bacteria were then re-suspended in PBS. The concentrated supernatants and bacterial suspension were separated by SDS-PAGE, followed by western blot analysis with mouse anti-His tag antibody and anti-Flag tag antibody (TransGen) to evaluate the expression and lysis-mediated release of CDPE and ColG. To investigate the cytotoxicity of bacterial culture medium, bacteria were centrifuged after 12 h of L-arabinose incubation. The bacterial culture supernatants were filtered through 0.22 μm filters and diluted tenfold in complete RPMI-1640 medium. 4T1 cells were seeded in 96-well plates at a density of 2500 cells/well and treated with the diluted bacterial culture supernatants for 48 h at 37 °C. The cytotoxic activity was measured by the above-described CCK-8 method. Masson's trichrome staining was used to reflect the effect of bacterially released ColG on collagen degradation within the TME. 4T1 tumor-bearing mice received intravenous injections every 3 days with PBS, EcN or EcN ColG (5×10^6 CFU in 100 μl PBS per mouse). The *LysE* gene was induced by intraperitoneal administration of L-arabinose (0.3 g/kg) 48 h post injection. On day 15, the mice were sacrificed. The paraffin sections of collected tumors were prepared and stained with a Masson's trichrome kit (Servicebio). In addition, these sections were imaged under a microscope (Nikon). The area ratios of collagen fibers were measured by Image J.

4.10. In vivo biodistribution and biosafety of EcN

When tumors reached approximately 100 mm^3, 4T1 tumor-bearing mice were injected intravenously with EcN CDPE or EcN ColG (5×10^6 CFU in 100 μl PBS per mouse). Tumors and major organs were homogenized using a tissue homogenizer (Servicebio) at 24 h post injection. Serial dilutions of homogenates were plated on LB agar plates at 37 °C overnight. Colonies were counted and computed as CFU/g of tissue. To determine the in vivo dynamics of EcN, EcN lux was injected intravenously into 4T1 tumor-bearing mice. The bacterial bioluminescence of mice was imaged at multiple time points over 3 days with IVIS (PerkinElmer). For short-term biosafety evaluation, 4T1 tumor-bearing mice received intravenous injections with PBS, EcN, EcN CDPE or EcN ColG (5×10^6 CFU in 100 μl PBS per mouse), and the blood serum was collected for hepatic function and inflammatory cytokine analysis after

24 h and 48 h of treatment. For long-term biosafety evaluation, 4T1 tumor-bearing mice received intravenous injections with PBS, EcN, EcN CDPE or EcN ColG (5×10^6 CFU in 100 μl PBS per mouse) every 3 days. On day 15, major organs were collected for HE staining.

4.11. In vivo antitumor effect

Antitumor treatments were performed using 4T1 tumor-bearing mice. When tumors reached a volume of approximately 60–100 mm^3, mice were randomly divided into different treatment groups. Overnight cultures of bacteria strains were diluted 100-fold into LB medium and grown to an OD_{600} of ~0.4. After centrifugation, the bacteria were washed with sterile PBS and adjusted to obtain a working concentration of 5×10^7 CFU/ml in PBS, with a total volume of 100 μl injected per mouse. For bacterial therapy experiments, mice were intravenously injected with PBS, EcN, EcN CDPE, EcN ColG or EcN Mix (EcN CDPE and EcN ColG at a ratio of 1:1) every 3 days. L-arabinose (0.3 g/kg) was intraperitoneally injected at 48 h post bacteria injection to induce the lysis-dependent release of therapeutic proteins. For combination chemotherapy, mice were intravenously injected with PBS, EcN, or EcN ColG every 3 days. Collagenase ColG was induced by intraperitoneal administration of L-arabinose (0.3 g/kg) at 48 h post bacteria injection. Then, the animals were intravenously injected with saline or doxorubicin (5 mg/kg) 3 h after protein expression induction. On day 15, tumors from each group were isolated and analyzed. Tumors in all groups were homogenized, and the homogenate supernatants were analyzed for IFN-γ by ELISA. Ki67 assays of tumor sections were conducted to detect tumor proliferation, and Masson's trichrome staining investigated the content of collagen fibers after bacterial therapy. Quantitative analysis of Ki67 positive cells and collagen fibers in the tumor areas was measured by Imgae J. To observe tumor accumulation of doxorubicin, L-arabinose (0.3 g/kg) was intraperitoneally injected into 4T1 tumor-bearing mice at 48 h post intravenous injection of PBS, EcN or EcN ColG (5×10^6 CFU). At 3 h after injection, doxorubicin at a dose of 5 mg/kg was intravenously injected into mice. The mice were sacrificed 1 h later, and tumors were isolated, frozen and cut into slices. The tumor accumulation of doxorubicin was observed by fluorescence microscopy and analyzed by Image J.

4.12. Statistical analysis

Statistical analysis was performed in GraphPad Prism. Unpaired Student's t-test, one-way ANOVA and two-way ANOVA were performed as appropriate. For Kaplan-Meier survival experiments, we performed log-rank (Mantel-Cox) tests. Details of the statistical tests are specified in the corresponding figure legends. Unless otherwise stated, experiments were conducted in biological replicates, with at least three replicates. Data are shown as mean ± s.e.m.

Notes

The authors declare no competing financial interest.

CRediT authorship contribution statement

Hong-Rui Li: Writing – review & editing, Writing – original draft, Validation, Conceptualization. **Bang-Ce Ye:** Writing – review & editing, Conceptualization.

Declaration of competing interest

The authors declare that they have no known competing financial interests or personal relationships that could have appeared to influence the work reported in this paper.

Acknowledgments

This work was sponsored by the National Natural Science Foundation of China (22134003) and the National Key Research and Development Program of China (2020YFA0908800).

Appendix A. Supplementary data

Supplementary data to this article can be found online at https://doi.org/10.1016/j.synbio.2024.09.001.

References

[1] Bray F, Laversanne M, Sung H, Ferlay J, Siegel RL, Soerjomataram I, et al. Global cancer statistics 2022: GLOBOCAN estimates of incidence and mortality worldwide for 36 cancers in 185 countries. CA Cancer J Clin 2024;74:229–63. https://doi.org/10.3322/caac.21834.
[2] Li M, Zhang Y, Zhang Q, Li J. Tumor extracellular matrix modulating strategies for enhanced antitumor therapy of nanomedicines. Mater Today Bio 2022;16. https://doi.org/10.1016/j.mtbio.2022.100364.
[3] Fleming JM, Yeyeodu ST, McLaughlin A, Schuman D, Taylor DK. In situ drug delivery to breast cancer-associated extracellular matrix. ACS Chem Biol 2018;13:2825–40. https://doi.org/10.1021/acschembio.8b00396.
[4] Yu T, Zhang G, Chai X, Ren L, Yin D, Zhang C. Recent progress on the effect of extracellular matrix on occurrence and progression of breast cancer. Life Sci 2023;332. https://doi.org/10.1016/j.lfs.2023.122084.
[5] Netti PA, Berk DA, Swartz MA, Grodzinsky AJ, Jain RK. Role of extracellular matrix assembly in interstitial transport in solid tumors. Cancer Res 2000;60:2497–503.
[6] Huo D, Jiang X, Hu Y. Recent advances in nanostrategies capable of overcoming biological barriers for tumor management. Adv Mater 2019;32. https://doi.org/10.1002/adma.201904337.
[7] Eikenes L, Bruland YS, Brekken C, Davies CDL. Collagenase increases the transcapillary pressure gradient and improves the uptake and distribution of monoclonal antibodies in human osteosarcoma xenografts. Cancer Res 2004;64:4768. https://doi.org/10.1158/0008-5472.CAN-03-1472.
[8] García-Olmo D, Villarejo Campos P, Barambio J, Gomez-Heras SG, Vega-Clemente L, Olmedillas-Lopez S, et al. Intraperitoneal collagenase as a novel therapeutic approach in an experimental model of colorectal peritoneal carcinomatosis. Sci Rep 2021;11. https://doi.org/10.1038/s41598-020-79721-0.
[9] Li J, Gong C, Chen X, Guo H, Tai Z, Ding N, et al. Biomimetic liposomal nanozymes improve breast cancer chemotherapy with enhanced penetration and alleviated hypoxia. J Nanobiotechnol 2023;21. https://doi.org/10.1186/s12951-023-01874-7.
[10] Diop-Frimpong B, Chauhan VP, Krane S, Boucher Y, Jain RK. Losartan inhibits collagen I synthesis and improves the distribution and efficacy of nanotherapeutics in tumors. Proc Natl Acad Sci USA 2011;108:2909–14. https://doi.org/10.1073/pnas.1018892108.
[11] Dolor A, Szoka FC. Digesting a path forward: the utility of collagenase tumor treatment for improved drug delivery. Mol Pharm 2018;15:2069–83. https://doi.org/10.1021/acs.molpharmaceut.8b00319.
[12] Wu T, Zhu J. Recent development and optimization of pseudomonas aeruginosa exotoxin immunotoxins in cancer therapeutic applications. Int Immunopharm 2021;96. https://doi.org/10.1016/j.intimp.2021.107759.
[13] Havaei SM, Aucoin MG, Jahanian-Najafabadi A. Pseudomonas exotoxin-based immunotoxins: over three decades of efforts on targeting cancer cells with the toxin. Front Oncol 2021;11. https://doi.org/10.3389/fonc.2021.781800.
[14] Weldon JE, Pastan I. A guide to taming a toxin – recombinant immunotoxins constructed from Pseudomonas exotoxin A for the treatment of cancer. FEBS J 2011;278:4683–700. https://doi.org/10.1111/j.1742-4658.2011.08182.x.
[15] He L, Yang H, Tang J, Liu Z, Chen Y, Lu B, et al. Intestinal probiotics E. coli Nissle 1917 as a targeted vehicle for delivery of p53 and Tum-5 to solid tumors for cancer therapy. J Biol Eng 2019;13. https://doi.org/10.1186/s13036-019-0189-9.
[16] Chowdhury S, Castro S, Coker C, Hinchliffe TE, Arpaia N, Danino T. Programmable bacteria induce durable tumor regression and systemic antitumor immunity. Nat Med 2019;25:1057–63. https://doi.org/10.1038/s41591-019-0498-z.
[17] Tumas S, Meldgaard TS, Vaaben TH, Suarez Hernandez S, Rasmussen AT, Vazquez-Uribe R, et al. Engineered E. coli Nissle 1917 for delivery of bioactive IL-2 for cancer immunotherapy. Sci Rep 2023;13. https://doi.org/10.1038/s41598-023-39365-2.
[18] Agrawal N, Bettegowda C, Cheong I, Geschwind J-F, Drake CG, Hipkiss EL, et al. Bacteriolytic therapy can generate a potent immuneresponse against experimental tumors. Proc Natl Acad Sci USA 2004;101. https://doi.org/10.1073/pnas.0406242101.
[19] Sasaki T, Fujimori M, Hamaji Y, Hama Y, Ito Ki, Amano J, et al. Genetically engineered Bifidobacterium longum for tumor-targeting enzyme-prodrug therapy of autochthonous mammary tumors in rats. Cancer Sci 2006;97:649–57. https://doi.org/10.1111/j.1349-7006.2006.00221.x.
[20] Murakami T, Hiroshima Y, Zhang Y, Zhao M, Kiyuna T, Hwang HK, et al. Tumor-targeting Salmonella typhimurium A1-R promotes tumoricidal CD8+ T cell tumor infiltration and arrests growth and metastasis in a syngeneic pancreatic-cancer orthotopic mouse model. J Cell Biochem 2017;119:634–9. https://doi.org/10.1002/jcb.26224.

[21] Zhao T, Wei T, Guo J, Wang Y, Shi X, Guo S, et al. PD-1-siRNA delivered by attenuated Salmonella enhances the antimelanoma effect of pimozide. Cell Death Dis 2019;10. https://doi.org/10.1038/s41419-019-1418-3.
[22] Phan TX, Nguyen VH, Duong MTQ, Hong Y, Choy HE, Min JJ. Activation of inflammasome by attenuated Salmonella typhimurium in bacteria-mediated cancer therapy. Microbiol Immunol 2015;59:664–75. https://doi.org/10.1111/1348-0421.12333.
[23] Zamboni DS, Kupz A, Curtiss R, Bedoui S, Strugnell RA. In vivo IFN-γ secretion by NK cells in response to Salmonella typhimurium requires NLRC4 inflammasomes. PLoS One 2014;9. https://doi.org/10.1371/journal.pone.0097418.
[24] Zhou S, Gravekamp C, Bermudes D, Liu K. Tumour-targeting bacteria engineered to fight cancer. Nat Rev Cancer 2018;18:727–43. https://doi.org/10.1038/s41568-018-0070-z.
[25] Ebelt ND, Zuniga E, Passi KB, Sobocinski LJ, Manuel ER. Hyaluronidase-expressing Salmonella effectively targets tumor-associated hyaluronic acid in pancreatic ductal adenocarcinoma. Mol Cancer Therapeut 2020;19:706–16. https://doi.org/10.1158/1535-7163.Mct-19-0556.
[26] Kim J-S, Park J-E, Choi S-H, Kang SW, Lee JH, Lee J-S, et al. ECM-targeting bacteria enhance chemotherapeutic drug efficacy by lowering IFP in tumor mouse models. J Contr Release 2023;355:199–210. https://doi.org/10.1016/j.jconrel.2023.02.001.
[27] Sockolosky JT, Dougan M, Ingram JR, Ho CCM, Kauke MJ, Almo SC, et al. Durable antitumor responses to CD47 blockade require adaptive immune stimulation. Proc Natl Acad Sci USA 2016;113. https://doi.org/10.1073/pnas.1604268113.
[28] Bannas P, Hambach J, Koch-Nolte F. Nanobodies and nanobody-based human heavy chain antibodies as antitumor therapeutics. Front Immunol 2017;8. https://doi.org/10.3389/fimmu.2017.01603.
[29] Ingram JR, Blomberg OS, Sockolosky JT, Ali L, Schmidt FI, Pishesha N, et al. Localized CD47 blockade enhances immunotherapy for murine melanoma. Proc Natl Acad Sci USA 2017;114:10184–9. https://doi.org/10.1073/pnas.1710776114.
[30] Antignani A, Ho ECH, Bilotta MT, Qiu R, Sarnvosky R, FitzGerald DJ. Targeting receptors on cancer cells with protein toxins. Biomolecules 2020;10. https://doi.org/10.3390/biom10091331.
[31] Kreitman RJ, Pastan I. Importance of the glutamate residue of KDEL in increasing the cytotoxicity of Pseudomonas exotoxin derivatives and for increased binding to the KDEL receptor. Biochem J 1995;307:29–37. https://doi.org/10.1080/01904169609365123.
[32] Chiang Z-C, Fang S, Shen Y-k, Cui D, Weng H, Wang D, et al. Development of novel CD47-specific ADCs possessing high potency against non-small cell lung cancer in vitro and in vivo. Front Oncol 2022;12. https://doi.org/10.3389/fonc.2022.857927.
[33] Deli MA, Syed F, Thomas AN, Singh S, Kolluru V, Emeigh Hart SG, et al. In vitro study of novel collagenase (XIAFLEX®) on dupuytren's disease fibroblasts displays unique drug related properties. PLoS One 2012;7. https://doi.org/10.1371/journal.pone.0031430.
[34] Kaushik S, Pickup MW, Weaver VM. From transformation to metastasis: deconstructing the extracellular matrix in breast cancer. Cancer Metastasis Rev 2016;35:655–67. https://doi.org/10.1007/s10555-016-9650-0.
[35] Holle AW, Young JL, Spatz JP. In vitro cancer cell–ECM interactions inform in vivo cancer treatment. Adv Drug Deliv Rev 2016;97:270–9. https://doi.org/10.1016/j.addr.2015.10.007.
[36] Dhillon S. Moxetumomab pasudotox: first global approval. Drugs 2018;78:1763–7. https://doi.org/10.1007/s40265-018-1000-9.
[37] Liang K, Liu Q, Li P, Han Y, Bian X, Tang Y, et al. Endostatin gene therapy delivered by attenuated Salmonella typhimurium in murine tumor models. Cancer Gene Ther 2018;25:167–83. https://doi.org/10.1038/s41417-018-0021-6.
[38] Chen QW, Wang JW, Wang XN, Fan JX, Liu XH, Li B, et al. Inhibition of tumor progression through the coupling of bacterial respiration with tumor metabolism. Angew Chem Int Ed 2020;59:21562–70. https://doi.org/10.1002/anie.202002649.
[39] Yu X, Lin C, Yu J, Qi Q, Wang Q. Bioengineered Escherichia coli Nissle 1917 for tumour-targeting therapy. Microb Biotechnol 2019;13:629–36. https://doi.org/10.1111/1751-7915.13523.
[40] Fang T-T, Zou Z-P, Zhou Y, Ye B-C. Prebiotics-controlled disposable engineered bacteria for intestinal diseases. ACS Synth Biol 2022;11:3004–14. https://doi.org/10.1021/acssynbio.2c00182.